Minimizing the climate impact of the next generation aircraft using novel climate functions for aircraft design

Radhakrishnan, Kaushik; Deck, K.T.; Proesmans, P.; Linke, Florian; Yin, F.; Grewe, V.; Vos, Roelof; Lührs, Benjamin; Niklaß, Malte; Dedoussi, I.C.

Publication date
2022

Document Version
Final published version

Published in
ICAS PROCEEDINGS 33th Congress of the International Council of the Aeronautical Sciences

33RD CONGRESS
OF THE INTERNATIONAL COUNCIL
OF THE AERONAUTICAL SCIENCES
STOCKHOLM, SWEDEN, 4-9 SEPTEMBER, 2022

ICAS 2022 SWEDEN

MINIMIZING THE CLIMATE IMPACT OF THE NEXT GENERATION AIRCRAFT USING NOVEL CLIMATE FUNCTIONS FOR AIRCRAFT DESIGN

K. Radhakrishnan[1], K. Deck[2], P. Proesmans[2], F. Linke[3], F. Yin[2], V. Grewe[2,4], R. Vos[2], B. Lührs[3], M. Niklaß[3] & I. Dedoussi[2]

[1]Institute of Air Transportation Systems, Hamburg University of Technology, Blohmstraße 20, 21079, Hamburg, Germany
[2]Delft University of Technology, Kluyverweg 1, 2629HS, Delft, The Netherlands
[3]Air Transportation Systems, German Aerospace Center, Blohmstraße 20, 21079, Hamburg, Germany
[4]Institute of Atmospheric Physics, German Aerospace Center, Oberpfaffenhofen, 82234, Weßling, Germany

Abstract

The aircraft's environmental performance on fleet level is so far completely decoupled from the design process. The climate impact from aviation arising from non-CO_2 effects are largely independent from CO_2 emissions, but rather depend on the atmospheric state. Previously complex climate-chemistry models were used to evaluate the non-CO_2 emissions impact on climate. This is far too computationally demanding for a multidisciplinary design optimisation (MDO) process, requiring a multitude of climate impact evaluations. The question then is, how to efficiently design the next generation climate optimal aircraft?

In this paper, a new concept for designing aircraft with minimum climate impact using Climate Functions for Aircraft Design (CFAD) is presented. The content of this paper provides an overview of the development of these innovative CFAD and demonstrates the ability to be integrated in an existing MDO framework. The mitigation potential by optimising aircraft design using CFAD is analysed with respect to different cruise conditions and by minimizing the overall climate impact. To validate the CFAD, a higher fidelity assessment is carried out. Finally, the key performance indicators, i.e. fuel consumption, flight time and operating cost, of the optimised aircraft design are compared to that of the reference aircraft.

Keywords: Aircraft design, Climate functions, CFAD, Multidisciplinary design optimisation, Climate impact

1. Introduction

With commercial aviation growing at an impressive pace, it is imperative to rethink the ways in which aircraft are designed and operated to lower the climate impact of aviation. Analysing the climate impact of aviation requires the consideration of interactions between aircraft, routings and atmosphere. Aircraft design optimisation studies often use fuel burn, maximum take-off mass, or direct operating cost as the objective function. However, when an environmental-impact metric is used, such as equivalent CO_2 emissions, the optimal aircraft has different wing-loading and thrust-to-weight ratio and flies at a different cruise altitude compared to an aircraft designed for minimal fuel burn, as shown in [1]. Around two-thirds of the climate impact from aviation arises from non-CO_2 effects, which include for example NO_x, water vapour and soot emissions, as well as contrail and contrail-cirrus formation [2]. Hence, it is essential to consider these non-CO_2 effects when developing optimised aircraft designs or when evaluating new technologies. Without considering the relevant route network and typical operating conditions, the current aircraft design process is decoupled from their environmental performance.

The non-CO_2 effects are largely independent from CO_2 emissions, their climate impact largely depend on the atmospheric state. Complex climate-chemistry models used in the past [3, 4, 5] to evaluate the climate impact of aircraft designs are far too computational demanding for a multidisciplinary optimisation, requiring multitude of climate impact evaluations. In this context, the project

"Global-warming-optimized aircraft design" (GLOWOPT) is set directly to address this challenge by developing novel climate functions which can be used by aircraft designers in combination with conventional aircraft design synthesis or MDO methods. The concept of Climate Change Functions (CCFs) was originally developed in the EU project REACT4C [6, 7] and extended to so-called algorithmic CCFs (aCCFs) in the SESAR Exploratory Research project ATM4E [8]. In these projects, three-dimensional (latitude, longitude, and altitude) CCFs were used to determine the optimum route or trajectory of an aircraft, as they allow for the computation of the climate impact of a unit emission of the relevant species (CO_2, H_2O, NO_x), which is released at a specific location. The objective behind the development of CCFs was to minimize the climate impact by optimising the flight trajectory for a fixed aircraft type. In comparison to that, the proposed Climate Functions for Aircraft Design (CFAD) describe in detail the climate impact of spatially varying emissions depending on the key parameters which are affected by aircraft design. CFAD are not a function of the location anymore but include the effect of the route network the aircraft are operated in implicitly. CFAD are novel as they contain fleet-level information in an aggregated way.

The objective of this paper is to present the Climate Functions for Aircraft Design as an easy-to-use tool which can be integrated into the existing aircraft synthesis framework. By minimizing these CFAD in the aircraft design optimisation process, a design solution can be synthesized with lower climate impact while considering the operating regime and the relevant market segment.

2. Concept of Climate Functions for Aircraft Design

To develop the CFAD for aircraft design optimisation, it is important to select a climate metric which can reliably represent the climate impact of different emission species. Furthermore, the calculation of the CFAD needs to address the key input parameters at the aircraft design level and needs a common interface with the multidisciplinary design optimisation (MDO) modelling chain. This section addresses the determination of the climate metric that can adequately represent the climate impact of the new aircraft design and describes the development strategy for the CFAD.

2.1 Climate Metric

Climate metrics quantify the climate impact. It is important to specify what "climate impact" means in the considered situation [9]. Various species contribute to the climate impact and have to be addressed adequately. In this study, the following species are considered for aviation: carbon dioxide CO_2, nitrogen oxides NO_x (which affects methane CH_4, ozone O_3, and primary mode ozone [PMO]), water vapour H_2O, and contrails [2]. Since these species have different lifetimes, the climate metric together with a time horizon puts a different weight on them depending on the choice. Therefore, it is important to carefully choose the most suitable climate metric for the considered case [10].

The most common climate metrics are Radiative Forcing, Global Warming Potential, Global Temperature Potential, and Average Temperature Response [9]. The Radiative Forcing gives a radiation change based on a concentration change of chemical elements in the atmosphere, while the Global Warming Potential is using the sum of these radiation changes up to a chosen time horizon [9]. This time horizon is chosen on subjective considerations, but the choice is quite important since it shifts the focus on long-lived or short-lived emissions and effects [10]. A disadvantage of the Radiative Forcing and the Global Warming Potential is that they are not addressing the temperature change directly [9]. Therefore, other metrics are used such as the Global Temperature Potential. This metric gives the temperature change resulting from the changes in radiation at a certain point in time, hence heavily relying on the time horizon. With the Average Temperature Response, the dependency on the time horizon is reduced, since it is an average temperature over the considered time horizon [9].

The choice of the best suited climate metric depends on the exact question which should be answered to be able to address the "climate impact" adequately. After the definition of the actual problem, an emission scenario can be chosen, with the principle possibilities of a pulse, a constant, or a freely defined scenario (e.g., increasing or decreasing emissions). The actual climate metric (e.g., Radiative Forcing, Global Warming Potential, Global Temperature Potential, Average Temperature Response) is then chosen based on the definition of the objective as well. The last point which has to be addressed is the choice of the time horizon [9]. Here, we are addressing the evaluation of new technology. Since it is estimated that new (aircraft) technology will be used for a longer period and

with a growing fleet in service, a rising emission scenario is applied. The climate impact will then be evaluated over a significant long enough period to gain full insight to the possible improvements of the new technology. With the Average Temperature Response, a direct connection to the temperature change can be drawn. Therefore, the Average Temperature Response with a time horizon of 100 years (ATR_{100}) is used in this study.

2.2 CFAD Development Methodology

Changing an aircraft design directly influences the flight performance and the flight mission profile. To address the non-CO_2 emissions impact on climate, the climate functions need to include the effect of the route network on which the new aircraft will be operated. For the CFAD development, emission inventories are calculated for various mission profile parameters, e.g., cruise altitude, climb angle, descent angle etc., which determine the location of the emissions released and are influenced by the aircraft design parameters. The mission profiles are developed as generic mission profiles comprising of climb phase, cruise phase with a continuous climb, and a descent phase. To ensure adequate accuracy in computing climate impact and to reduce complexity of the CFAD, the generic mission profiles are generated assuming combinations of different final cruise altitudes and climb angles. The climb angle during cruise and descent angle are assumed constant. The emission inventories are calculated by mapping these generic mission profiles on the great circle trajectory for each route in the route network. The emissions contained within these emission inventories are based on the average fuel consumption per km of the reference aircraft mission profiles, calculated using the Trajectory Calculation Module [11] for different mission lengths.

The CFAD are then generated as a response surface model which is calculated with the atmospheric data and emission inventories, using the climate model AirClim [12]. AirClim is designed to specifically evaluate the climate impact of aircraft. Therefore, climate impact from specific climate agents i.e. CO_2, H_2O, CH_4, O_3, PMO (Primary Mode Ozone), and contrails is analysed for the route network [12, 13]. The CFAD are represented as a 4D response surface, which includes the final cruise altitude, climb angle, flight phase and climate agent.The CFAD response surface can be integrated within the MDO framework via an interface which determines the two mission profile parameters in every iteration of the MDO process. Using interpolation methods, the ATR_{100} from each climate agent for all three flight phases can be computed. The ATR_{100} is then scaled to the actual emissions of the aircraft to obtain the climate impact of the new design. The schematic representation of the CFAD development and integration with the MDO process is shown in Figure 1.

The objective of the CFAD developed and utilised in this paper is to study the general methodology and associated limitations. In the future, the CFAD will be updated with more adequately chosen scenarios and improved computational methods. Emission inventories were generated for final cruise altitudes corresponding to flight level 150, 200, 250, 300, 350, 400, and 450, and for average climb angles of 0.5°, 1.5°, 2.5°, 4.0°, and 5.0°. The generated CFAD are based on the climate metric ATR_{100}, and are represented in Figure 2 relative to the ATR_{100} corresponding to final cruise flight level 450 and climb angle 5°. A representative route network from year 2019, discussed further in Section 3, is considered for the emission inventories calculations. It is assumed that the route network follows a rising emission scenario considering the temporal scale. The overall simulation period is from 1940 up to 2150. The IPCC Fa1 scenario (developed by ICAO Forecasting and Economic Support Group [FESG]) [14] represents an increasing scenario and is therefore applied here with a normalization in 2050 which represents the full considered fleet size in this year. The ATR_{100} is calculated from 2050 up to 2150. AirClim evaluates the emission inventory against a given background scenario, in this case, SRES A1B [15].

Figure 2 illustrates the dependency of the ATR_{100}, all flight phases combined, for combinations of climb angle and final cruise altitude. It is important to note that the plots show dependencies contained within the CFAD and do not represent the actual climate impact. The actual ATR_{100} values for any combination of the mission profile parameters can be obtained by scaling the CFAD with the corresponding aircraft emissions. By varying the climb angle the flight path vis-à-vis the emission location is altered, and also the time spent in the cruise phase is altered. This results in a direct dependency between climb angle and climate impact. This is clearly visible in the case of contrails. For contrails, shown in Figure 2b, a peak of the ATR_{100} can be observed at a final cruise altitude of

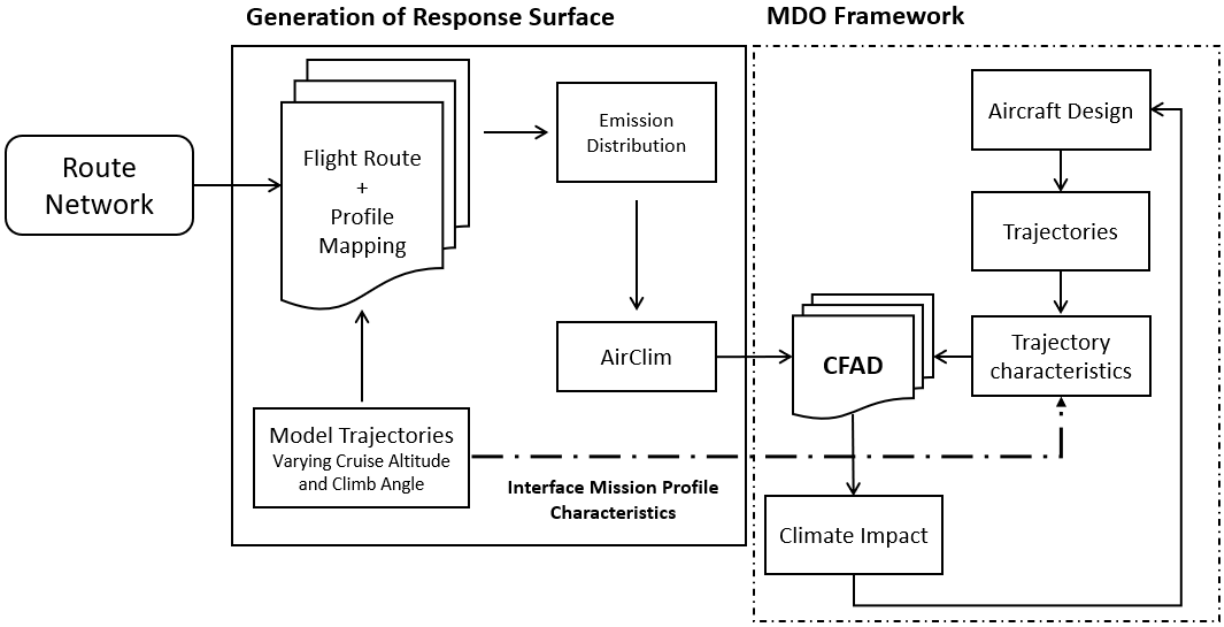

Figure 1 – Development methodology of the CFAD response surface model and the interface representation with MDO framework.

flight level 400. This is in line with the most suitable atmospheric conditions for contrail formation. With increasing climb angle the cruise phase becomes longer and thus the high impact from contrails can be observed to become more prominent at higher altitudes. The impact of the NO_x emissions is shown in Figure 2c. A strong dependency on altitude can be observed, increasing ATR with increasing cruise altitude. This impact combines effects of CH_4, O_3, and PMO. The individual effects from each of the latter species have varying levels of dependency on the mission profile parameters which are captured within the CFAD.

3. Top-Level Requirements and Reference Route Network

Most aircraft design studies focus on minimizing the operating cost of standard design missions while fulfilling certain TLARs and design constraints. However, the aircraft's environmental performance requires the knowledge of typical operating conditions, the potential market to be covered, and information on the routes to be operated on. In this section, we identify the design requirements for the next generation air transport category aircraft that minimize the global warming impact of aircraft fleets, while still offering flexibility to airlines to compete in the selected market segments.

An overview of the required transport capacities on any flight capacity i.e., flight frequencies, aircraft size and passenger demand, in conjunction with technological and infrastructure constraints will constitute the basis for identifying the relevant TLARs and design constraints. AIRCAST [16], an air traffic forecast model is used to model the growth of the passenger flow and aircraft movements over time. The list of requirements studied contains the cruise altitude, Mach number, take-off field length, wingspan, seating capacity, and approach speed. Through analyses of the current and future requirements, existing airport infrastructure and literature review of the operational conditions required for minimising the climate impact, the TLARs are defined. The bounds imposed on the cruise altitude and Mach number are based on the lower and upper bounds identified in [17]. A summary of the design requirements is given in Table 1. Further requirements regarding the loiter time, reserve fuel strategy, and limiting parameters from a certification point of view are defined to adhere to regulations.

Multiple studies [18, 19, 20, 21] have demonstrated higher potential in lowering the non-CO_2 effects on climate impact by flying at a lower cruise altitude and reduced speed. However, the location dependency of the non-CO_2 emissions could vary the optimal cruise conditions depending on the region where the aircraft is operated. The study of Dahlmann et al. [22] presents an overview of the variation in the optimal combinations of cruise altitude and Mach number by computing route-specific

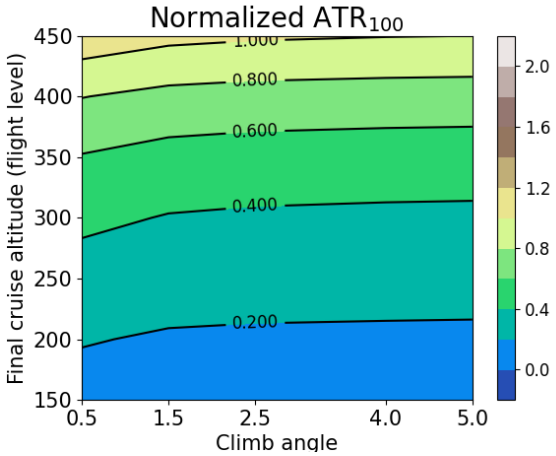

(a) Total ATR_{100} (for all considered species together)

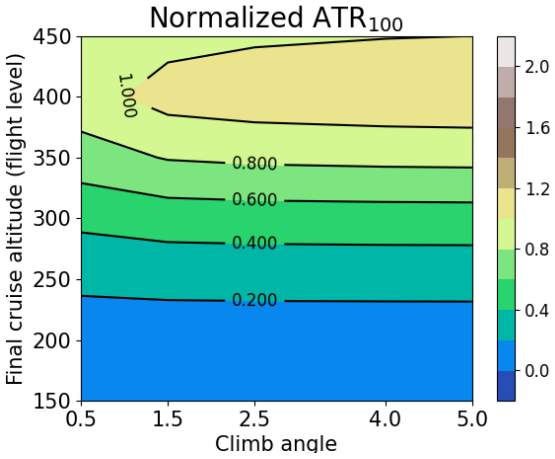

(b) ATR_{100} for contrails

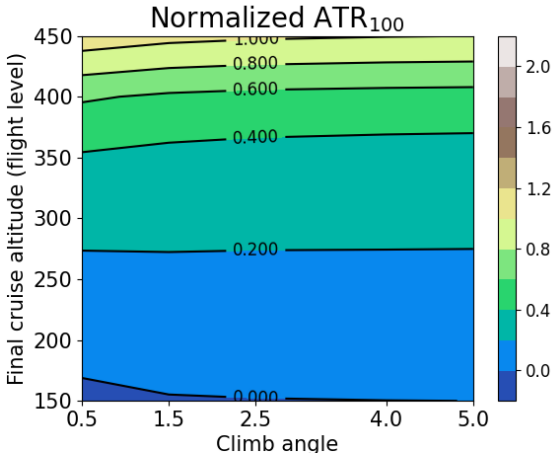

(c) ATR_{100} for NO_x emissions (combination out of CH_4, O_3, and PMO)

Figure 2 – ATR_{100} Response Surface (normalized with the corresponding value for flight level 450 and climb angle 5°) based on the reference aircraft emission inventories created as function of the final cruise altitude and the climb angle.

Table 1 – Summary of top-level requirements for GLOWOPT aircraft design.

Variable [Unit]	**Constant**	**Lower Bound**	**Upper Bound**
Initial cruise altitude [m]	-	4000	12000
Mach number [-]	-	0.60	0.84
Range at design point [km]	14150	-	-
Take-off field Length (Sea Level) [m]	2700	-	-
Wingspan [m]	-	-	65
Passenger number at design point [-]	350	-	-
Cargo volume [kg/m^3]	0	-	-
Max seating capacity [-]	450	-	-
Standard mass (passenger + baggage) [kg]	100	-	-
Approach speed [m/s]	72	-	-

Pareto fronts. From [22] it can be derived that the climate optimal operating conditions are susceptible to the region of operation. Furthermore, the optimal cruise conditions would vary depending on the technology which is considered. Because the higher objective of developing CFAD is for application in designing all aircraft types (regional, long-haul flights and novel aircraft designs), it is recommended

to consider the cruise altitude and Mach number as design variables which are then computed within the design optimisation process.

The design mission is the point on the payload-range diagram which defines the fuel requirements of an aircraft. This is crucial for the design process. To address the design range, we need to first select a representative route network on which the climate-optimised aircraft is to be operated. For the purpose of this study, it was decided to consider the route network with highest contribution to the aviation related climate impact. A detailed analysis of the climate impact stemming from both CO_2 and non-CO_2 emissions was carried out to identify the overall contribution of different aircraft types, in terms of seat capacity, to global aviation related climate impact. We considered the 2012 air traffic data and corresponding route network for this analysis. Table 2 summaries aircraft seat categories considered and their contribution to climate impact, fuel and air-distance flown. It can be observed that aircraft with seat capacity larger than 252 seats (typical wide-body, long-range aircraft) contributes significantly to the overall climate impact relative to the air-distance flown. Further, from literature (e.g., [17, 20, 22, 21]) considerable climate mitigation potential can be identified for routes operated with long-range aircraft. Accordingly, it is determined that the route network operated by aircraft with more than 252 seats as the reference market segment. The Airbus A350-900 is selected as the reference aircraft for this market, which is the latest aircraft to enter into service in the selected seat category. For a comparative analysis, within the scope of GLOWOPT, two design ranges are selected, one similar to the reference aircraft and the other adapted to the mission lengths of the routes identified within the reference network. However, for the purpose of this paper, we present the design which has a range similar to the reference aircraft. The seating capacity and approach speed requirements of the next-generation aircraft are kept similar to that of the reference aircraft.

Table 2 – Contribution to climate impact (ATR), fuel consumption and air-distance flown by different aircraft seat categories operated in year 2012, from air traffic data predicted using AIRCAST.

Aircraft Seat Category	Climate Impact (%)	Fuel Consumption(%)	Air-Distance (%)
<50	2	2	7
50-150	25	23	33
151-251	34	36	41
252-600	39	39	19

For the take-off field length (TOFL) and wingspan requirements, the runway characteristics of airports in all Origin-Destination (OD) pairs from the selected market segment were analysed. For each airport, the physical runway length is obtained from an airport database and the corrected runway length is calculated using the approach given by ICAO [23]. The airport with the shortest runway at sea level is considered critical for deriving the TOFL. For the year 2019, the average daily temperature and hottest month are derived for each airport using the METAR data. Similar to the TOFL, the wingspan requirement is derived bearing the capability of the airport to be served. For each OD airport pair in the selected market, the width is obtained from an airport database. The critical airport is determined by comparing the widths of the longest runway of each OD pair and selecting the airport with the smallest runway width. Using the width information of the critical airports and the ICAO recommended wingspan limitation, an upper limit to the wingspan of 65 m is defined.

4. Multidisciplinary Aircraft Design optimisation

This section focuses on implementing the newly developed CFAD in a conceptual, multidisciplinary aircraft design and optimisation framework. The design methods are briefly introduced in Section 4.1. In Section 4.2, we examine the influence of mission variables on the climate impact, and in Section 4.3, a long-range aircraft is optimised for the requirements introduced in Section 3. In this study, the aircraft configuration is a traditional tube-and-wing configuration with two wing-mounted engines.

4.1 MDO Setup and Aircraft Design Methods

We use a multidisciplinary design framework to carry out design of experiments and MDO. The setup of the framework is presented in Figure 3 in the format of an extended design structure matrix. This setup demonstrates how the CFAD can be integrated into multidisciplinary workflows. The main inputs to the framework are the top-level aircraft requirements, which remain constant, and the design vector $\mathbf{x}$. This vector consists of nine variables which are gathered in Table 3 and target the airframe, engine cycle, and mission profile. Note that in the aircraft design process, we use the initial cruise altitude, whereas the final cruise altitude is used in the CFAD. In the MDO framework, the mission analysis ensures that a correct conversion is made between the two parameters.

Table 3 – Design variables and their respective bounds and reference values for the multi-disciplinary optimisation.

Variable [Unit]	Lower Bound ($\mathbf{x}^L$)	Reference ($\mathbf{x}^0$)	Upper Bound ($\mathbf{x}^U$)
Wing loading W/S [$\mathrm{kN/m^2}$]	6.00	6.31	8.03
Aspect ratio A [-]	8.00	9.50	12.0
Bypass ratio BPR [-]	5.00	9.60	11.0
Fan pressure ratio Π_{fan} [-]	1.1	1.55	1.80
LPC pressure ratio Π_{lpc} [-]	1.1	1.55	1.80
HPC pressure ratio Π_{hpc} [-]	10.0	22.2	25.0
Turbine entry temperature TET [K]	1100	1410	1700
Initial cruise altitude h_{cr} [km]	4.00	10.5	12.0
Cruise Mach number M_{cr} [-]	0.60	0.84	0.90

The aircraft design routine, which forms the framework core, takes this design vector and TLARs, and creates a consistent design in terms of mass and geometry [24]. Subsequently, a numerical mission analysis is performed to compute the emissions at various time steps and altitudes in the mission profile, as well as the average climb angle during the climb phase. This information is then passed on to step 6 to evaluate the CFAD. In the case of MDO, the CFAD provide the ATR_{100} value to the optimiser which proposes a new design vector.

The disciplines inside the aircraft design loop are based on statistical and physics-based methods [24]. The airframe module firstly determines the wing surface area and take-off thrust required, considering take-off length, cruise, and climb gradient constraints. Subsequently, a conceptual geometry of the aircraft is created. The fuselage is designed using an inside-out approach, following the passenger capacity requirements. The wing planform results from empirical rules [25, 26]. For the empennage sizing, we assume statistical tail volume coefficients from reference aircraft data. A quadratic drag polar is computed using this conceptual geometry. This drag polar consists of a lift-independent term, which is the sum of the minimum pressure drag contribution of the aircraft components, and a lift-dependent term which varies with the aspect ratio and Oswald factor. Finally, the airframe module assesses the operating empty mass (OEM) of the aircraft using Class-II mass estimation methods [25].

The propulsion step in the framework analyses the thermodynamic cycle in on- and off-design conditions of the turbofan engine and provides fuel consumption data to other disciplines. In addition, the propulsion discipline determines the mass of the two engines and estimates their length and diameter. The methods in this discipline are physics-based, employing the 1D modelling approach from Mattingly et al. [27] with a temperature-dependent specific gas model introduced in Walsh and Fletcher [28]. In the current study, we only examine kerosene-powered engines.

The mission analysis in step 4 of Figure 3 provides an update of the total fuel mass including reserve fuel to carry out diversion and loiter phases. The fuel mass and the updated OEM, from step 2, are added to the required payload mass to update the maximum take-off mass (MTOM). The converger continues until the MTOM and OEM have converged. In step 4, analytical expressions are used to estimate the fuel mass in cruise and contributions due to the take-off, climb, and reserve phases, according to the lost-range method [29]. In step 5, a physics-based, numeric mission anal-

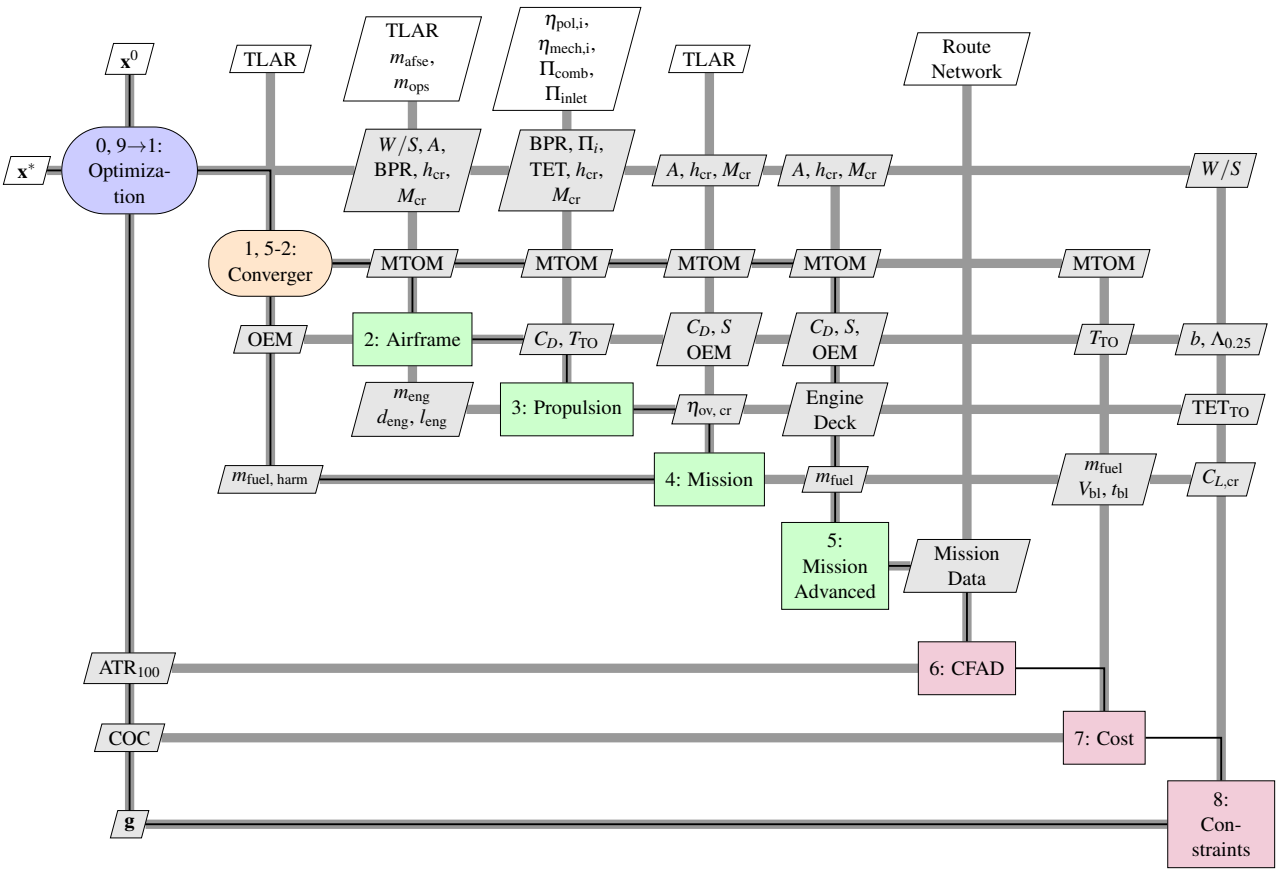

Figure 3 – Extended design structure matrix showing the multidisciplinary aircraft design workflow and integration of CFADs (adapted from [24]).

ysis is carried out to evaluate the performance and emissions at discrete time steps throughout the flight. This analysis is performed outside of the convergence loop to save computational time.

4.2 Influence of Cruise Altitude and Mach Number

Earlier studies [30, 22] have shown that mission variables, such as initial cruise altitude (h_{cr}) and cruise Mach number (M_{cr}), perform an important role in the climate impact of aircraft. The cruise altitude for example influences the climate impact of non-CO_2 climate agents, such as NO_x emissions [31] and contrails [32]. This is also confirmed by the analysis in Figure 2. Furthermore, the cruise altitude and Mach number drive the aircraft and engine design, which in turn affects the climate impact. In this section, the climate impact variation with respect to these two parameters is studied before initialising the MDO. We vary the initial cruise altitude h_{cr} between 6 and 11km, and the cruise Mach number M_{cr} between 0.6 and 0.84 (the reference value), while keeping all other design variables fixed to the reference values in Table 3. The aircraft is redesigned for each combination h_{cr} and M_{cr} before its climate impact is evaluated. This means that, among other differences, the wing sweep angle and the design point of the engine change.

The relative change in total ATR_{100} with respect to the reference aircraft is presented in Figure 4a. This figure shows that a 40% reduction in total ATR_{100} can be achieved by flying at an initial cruise altitude of 6.0km and a Mach number of 0.6. The trends in Figure 4a indicate that the altitude for which the total ATR_{100} is minimised, varies with the Mach number. This total ATR_{100} change is the sum of the contributions due to CO_2, H_2O, and NO_x emissions and the formation of contrails. The effect of h_{cr} and M_{cr} on these different species is shown in Figures 4b to 4d.

The contribution of CO_2 to ATR_{100} is minimised near the reference point, at Mach 0.84 and an altitude of 10.5km. Because the CO_2 emissions are directly related to the fuel burn, this operating point also minimises the fuel burn. When flying slower, the optimal cruise altitude decreases to maintain a near-optimal lift-to-drag ratio during the cruise phase. In addition, Figure 4b shows that

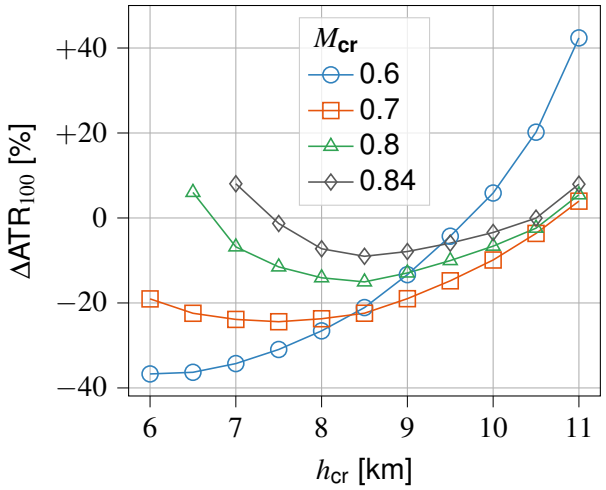

(a) Total ATR_{100} difference

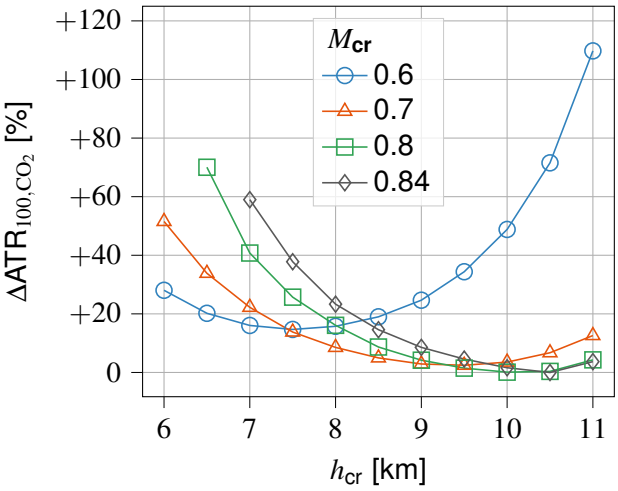

(b) Difference in ATR_{100} due to CO_2

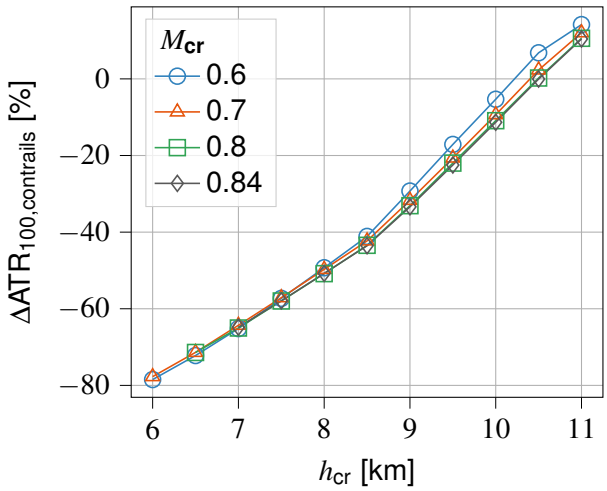

(c) Difference in ATR_{100} due to contrails

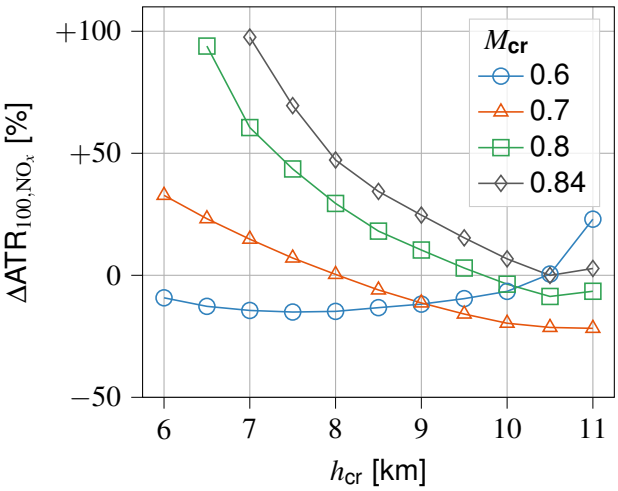

(d) Difference in ATR_{100} due to NO_x

Figure 4 – Variation in ATR_{100} contributions with initial cruise altitude h_{cr} and Mach M_{cr} number (the reference point is h_{cr}=10.5 km, M_{cr}=0.84)

the contribution due to CO_2 is higher at the point where the total ATR_{100} is minimised.

From Figure 4c, we can observe that the effects due to contrails significantly reduce by 80% when flying at 6.0km instead of 10.5km. This reduction is the largest contribution to the 40% decrease in overall ATR_{100}, as seen in Figure 4a. Furthermore, the ATR_{100} contribution due to contrails is nearly independent of the Mach number, in the current implementation of the CFAD.

The contribution due to NO_x, as presented in Figure 4d, is more complex; it is the sum of the heating effect due to an O_3 increase and the cooling effects due to methane and PMO depletion. At lower altitudes, the emission index of NO_x is higher due to the increased pressures and temperatures in the engine cycle. In addition, the aircraft performance and total fuel burn are affected by the selected Mach number. On the other hand, the indirect warming effects due to NO_x are reduced at lower cruise altitudes due to a shorter lifetime, as can be seen in Figure 2c. Hence, the trends shown in Figure 4d are the result of both the absolute emissions and the altitude effects. This highlights the importance of considering the aircraft and engine performance in the ATR_{100} evaluation.

The study in this section demonstrates how sensitive the aircraft climate impact is to the selected cruise altitude and Mach number. Additionally, Figure 4 highlights the importance of non-CO_2 effects in this assessment. While a significant climate impact reduction can be achieved by varying the mission parameters, the following section studies how the other design variables can further improve the climate impact.

4.3 Multidisciplinary Design optimisation

Due to the computational efficiency of the CFAD, they can be applied in the conceptual optimisation of aircraft. In this section, a long-range, wide-body aircraft is optimised for its climate impact, considering the route network and specifications mentioned in Section 3. We search the design vector which minimises the single-objective function ATR_{100} using the multidisciplinary framework introduced in Section 4.1. Additionally, four inequality constraints are added to bound the design space. These constraints consider the approach speed (max. 72m/s), the wing span (65m), the buffet lift coefficient, and TET in take-off condition (max. 2000K) [24]

Through numerical optimisation, an aircraft design is obtained which reduces the ATR_{100} by approximately 57% compared to the reference design that is similar to current cost- or fuel-optimal aircraft. Figure 5 shows how the individual contributions of ATR_{100} are varied to achieve this overall climate impact reduction. We observe that the largest climate impact reduction follows from a decrease in the contribution of non-CO_2 climate agents, namely short-lived ozone O_3, contrails, and water vapour (H_2O). On the other hand, the climate impact due to CO_2 increases by 8.8%.

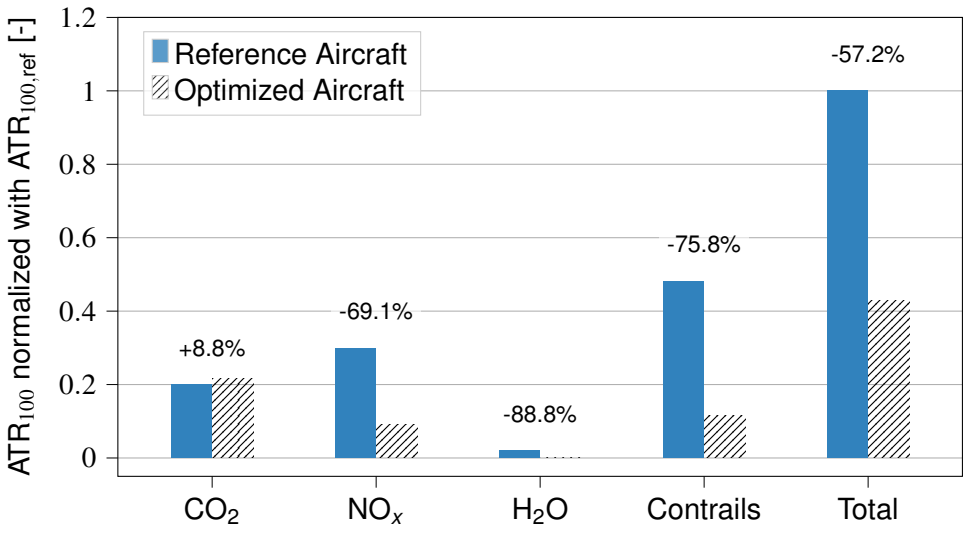

Figure 5 – Comparison of climate impact contributors between the reference and ATR_{100}-optimal aircraft

This reduction in ATR_{100} is achieved by varying the nine design variables introduced in Table 3. The optimised variables are presented in Table 4. Each category of variables influences the design and climate impact as follows: first, the climate-optimal aircraft cruises at a lower cruise altitude. The advantage of this design choice is that the impact of contrails is significantly reduced by 76% and the contribution of water is lowered by 89% due to the shorter lifetime of water vapour at lower altitudes. The relation between altitude and contrails was already identified in the experiment in the previous section, and it is clear that the optimiser makes use of this relation. The Mach number is varied accordingly to maximise the lift-to-drag ratio in cruise.

Second, the engine features a higher bypass ratio, but a lower overall pressure ratio (OPR). The OPR is reduced from 53.3 to 28.1, corresponding to a decrease of 47%. This design choice is counter-intuitive as a higher OPR leads to reduced fuel burn and, as a consequence, to lower CO_2 emissions. However, a lower OPR reduces the NO_x emission index, since this parameter is strongly dependent on the temperature and pressure in the combustor. This relation is modelled through the p3-T3 method used in this study [24]. Since the pressure throughout the engine cycle is increased at the lower cruise altitude, the optimiser minimizes the NO_x emissions by reducing the emission index, which in turn lowers the radiative effects due to ozone O_3. This preference can be explained by investigating Figure 5, which indicates that the contribution due to NO_x is initially larger than the CO_2 effect for the reference aircraft. Furthermore, a reduction in NO_x emissions can also be beneficial in terms of pollution, although a quantitative assessment of this effect is considered out of scope in this paper. However, reducing the NO_x emissions also lowers the absolute cooling effects present due to

Table 4 – Design variables of the reference aircraft and design variables which minimise the ATR of the aircraft

Variable [Unit]	Reference Value	Optimal Design	Difference
W/S [$\mathrm{kN/m^2}$]	6.31	8.03	+27%
A [-]	9.50	12.0	+26%
BPR [-]	9.60	10.8	+13%
Π_{fan} [-]	1.55	1.42	-5.5%
Π_{lpc} [-]	1.55	1.32	-12%
Π_{hpc} [-]	22.2	15.0	-33%
TET [K]	1410	1350	-4.2%
h_{cr} [km]	10.5	6.26	-40%
M_{cr} [-]	0.84	0.613	-27%

the depletion of methane and PMO.

Nevertheless, this design choice depends on the accurate estimation of the NO_x emission index EI_{NO_x}. Several methods exist to evaluate this parameter, depending on the pressure and temperature, but for example also on the fuel-to-air ratio. Hence, the results obtained through MDO can vary with the chosen relation to evaluate the NO_x emission index. Therefore, we recommend exploring the implementation of other relations for EI_{NO_x} and investigate the effect on the optimal engine design.

Finally, considering the airframe variables, the optimisation increases the aspect ratio and wing loading to the maximum achievable values. This trend is facilitated partially by the above design choices. The reduced Mach number eliminates the need for wing sweep to limit wave drag. This non-swept wing allows for a higher maximum lift coefficient $C_{L,\text{max}}$ (here 2.8) in landing configuration. The high $C_{L,\text{max}}$ value allows a high wing loading of 8.03 $\mathrm{kN/m^2}$ without violating the approach speed constraint. Furthermore, the high wing loading combined with the zero-sweep angle allow for a lighter wing with a shorter span. Therefore, the aspect ratio can be maximised without violating the span constraint of 65 meters. The high aspect ratio improves the cruise efficiency and limits the penalty in fuel burn and CO_2 contribution.

Figure 6 compares the top-view geometries of the reference and optimised aircraft. While the fuselage geometry remains unchanged, the wing planform changes due to reduced Mach number and larger wing loading and aspect ratio of the optimised aircraft. Although the engine of the optimised aircraft features a larger bypass ratio, the diameter is smaller due to the higher density at cruise altitude. The surface area of the horizontal tailplane is underestimated due to the conceptual method employed to determine the area. We assume a constant volume coefficient when designing the optimal aircraft. Because the main wing area is reduced, due to the higher wing loading, the area of the horizontal tail area automatically shrinks accordingly. Therefore, it is recommended to use a more advanced method in future optimisations. Nevertheless, if we consider that the tail area would be equal to the reference aircraft, the maximum achievable difference in total ATR_{100} would be 1% smaller, mostly due to increased fuel burn and CO_2 emissions. The effect of this constant volume coefficient on the final climate impact thus appears to be limited.

In conclusion, lower and slower flight in combination with a lower engine pressure ratio can significantly reduce the climate impact due to contrails, water vapour, and nitrogen oxides. This analysis is completed with fossil kerosene and currently available technology levels. A logical next step is to use the CFAD in an assessment of future technologies to evaluate further improvements.

5. Validation and Performance Assessment

In order to assess the effectiveness and validate the CFAD for the aircraft design process, a detailed higher fidelity assessment is conducted using GRIDLAB [33] and AirClim. GRIDLAB is a tool developed for the environmental analysis of new technologies and operational concepts for aviation. In this section, we investigate the climate impact of the reference aircraft based on the flight performance calculated using the design setup described in Section 4.1 and from the BADA 4 performance model

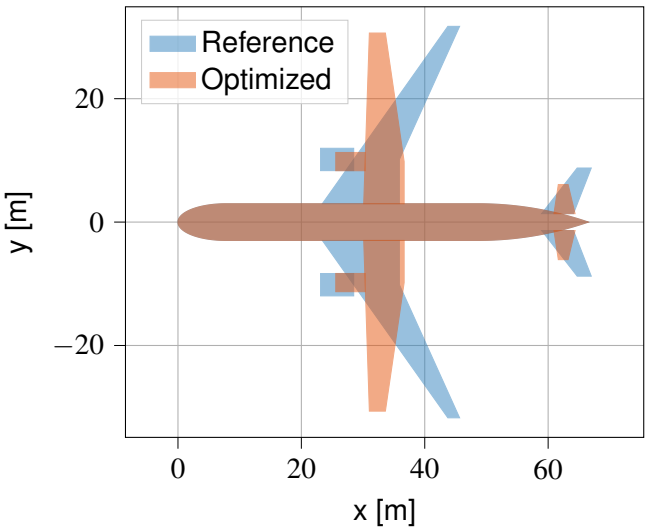

Figure 6 – Top-view comparison of reference and optimised aircraft

[34]. We then compare the ATR_{100} values estimated by the higher fidelity toolchain and CFAD. Finally, comparative studies are conducted for performance indicators such as fuel consumption, flight time and operating cost for the reference aircraft and climate optimised aircraft design discussed in Section 4.3.

5.1 Higher Fidelity Assessment

A higher fidelity toolchain is set up to calculate detailed trajectories for the route network defined in Section 3. The resulting emission distribution along each route of the route network is aggregated as emission inventories using GRIDLAB. Based on the trajectory calculation and emission inventories the climate impact assessment is carried out using the AirClim.

For the validation of the CFAD, two performance models are selected for the reference aircraft. The detailed trajectory calculation and emission inventories for the reference aircraft based on the BADA performance model[35] ($BADA_{Ref.}$) and the flight performance determined using the MDO toolchain ($GLOWOPT_{Ref.}$). The climate impact for the reference aircraft based on both performance models is calculated using the AirClim climate model and CFAD. The reference aircraft are flown at different flight levels to investigate the CFAD accuracy in estimating the ATR with different operating conditions. Figure 7 shows the total ATR_{100} estimated using the higher fidelity assessment (HFA) model ($BADA_{Ref.,HFA}$, $GLOWOPT_{Ref.,\ HFA}$) and CFAD ($BADA_{Ref.,CFAD}$, $GLOWOPT_{Ref.,\ CFAD}$) at flight levels 200, 300 and 400. The ATR values are represented relative to the $ATR_{100,ref}$ of $GLOWOPT_{Ref.,\ HFA}$ at flight level 400 (the reference aircraft climate impact at its typical cruise altitude). It can be observed that there is a difference in the total climate impact within the higher fidelity setup between the two performance models. The climate impact assessed for the $GLOWOPT_{Ref.,\ HFA}$ is lower in comparison to $BADA_{Ref.,HFA}$. The ATR difference between the two performance models increases from 2% at flight level 200 to 21% at flight level 400. The total ATR values are underestimated by the CFAD for both performance models relative to the higher fidelity ATR. At flight level 200, the ATR estimated by the CFAD is 3% lower for the BADA performance model and 4% for the reference aircraft. As the flight cruise altitude is increased, the ATR between the higher fidelity and CFAD differ by 6% and 7% at flight level 300 and 14% and 15% at flight level 400 for both performance models respectively.

In Table 5, we can observe the percentage difference between the higher fidelity and CFAD ATR_{100} values for each individual climate agent. The negative sign indicates that the ATR value is underestimated by the CFAD. The CFAD ATR values for all climate agents (except Ozone) are estimated with an error margin well under 5% for all flight levels. The major contributor to the inaccuracy at higher altitudes observed can be attributed to ozone. The error in estimating the effects of ozone grows exponentially with flight cruise altitude, with maximum errors of 13% and 11.3% at flight level 400 for $BADA_{Ref.}$ and $GLOWOPT_{Ref.}$ respectively. Since effects of ozone are predominant at higher altitudes, the overall inaccuracy of CFAD increases at higher altitudes. This suggests that the emission distri-

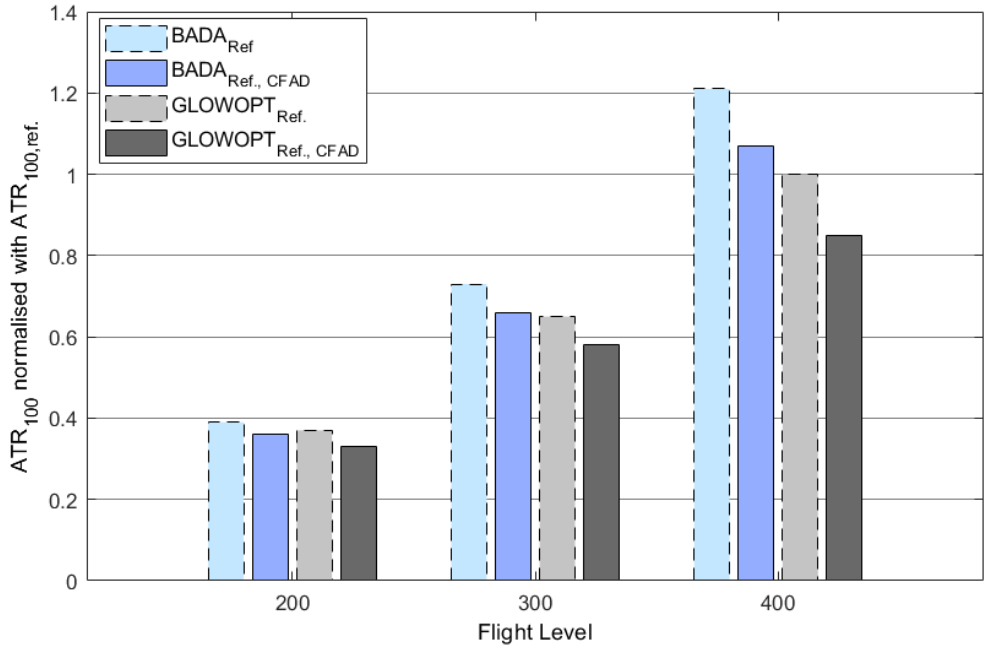

Figure 7 – Comparison of $ATR_{100,Total}$ for the reference aircraft using BADA performance model and GLOWOPT MDO toolchain, evaluated using higher fidelity setup and CFAD.

butions at higher altitudes are not captured accurately within the CFAD. Minor improvements in the results can be expected by improving the consistency of the assumptions involved in the calculation of the trajectories by GRIDLAB and the generic trajectories developed within the CFAD. For example, the detailed trajectories calculated by GRIDLAB presently consider constant altitude cruise phase, while the generic trajectories of CFAD consider continuous climb during cruise.

Table 5 – Comparison of ATR_{100} for individual species for the reference aircraft from BADA performance model and GLOWOPT MDO toolchain, evaluated using higher fidelity setup and CFAD.

Emitted Species	**$BADA_{Ref.}$**			**$GLOWOPT_{Ref.}$**		
	FL-200	FL-300	FL-400	FL-200	FL-300	FL-400
Carbon dioxide (CO_2)	-0.07%	-0.73%	-0.14%	-0.01%	-0.54%	0.49%
Water Vapour (H_2O)	-0.01%	-0.15%	-2.41%	-0.01%	-0.13%	-1.51%
Ozone (O_3)	-1.90%	-3.78%	-13.01%	-1.59%	-4.33%	-11.31%
Methane (CH_4)	-0.06%	0.17%	0.79%	-0.53%	0.89%	0.69%
Contrails	-1.25%	-2.44%	0.51%	-1.26%	-2.45%	-3.05%
Primary Mode Ozone (PMO)	-0.02%	0.06%	0.27%	-0.18%	0.30%	0.23%

Improving the accuracy of the CFAD is an iterative process. Currently, further developments to the CFAD are underway. A step forward would include scrutiny of the assumptions involved in the development of generic trajectories and the interpolation techniques considered within the CFAD development methodology, e.g. increasing the number of flight levels considered at high altitudes since the overall climate impact is highly sensitive at high altitudes (see figure 2). Additionally, assessments of the effectiveness of CFAD to evaluate new technologies will be carried out and different emission scenarios will be considered. However, the interim results described in this paper indicate that, CFAD are able to estimate the climate impact of an aircraft design with reasonable error at low altitudes. At high altitudes, CFAD is able to capture the overall effects of different emission species, but further analysis needs to be carried out to improve the fidelity of CFAD at high altitudes.

5.2 Performance Indicators and Cost Assessment

In this section, we consider the key performance indicators and economic targets which are historically considered when developing new aircraft designs. Since designing a climate-optimal aircraft results in changes in operating conditions, we compare the fuel consumption, flight time and operating cost of the climate-optimised aircraft design to that of the reference design. For operating cost we consider the Cash-Operating Cost (COC), which includes the costs of fuel, crew, landing fees, navigation charges and maintenance, and the Direct-Operating Cost (DOC), which combines the COC, depreciation cost (airframe and engine), and insurance charges. The COC and DOC estimated in this section are derived from using the method described in [36].

Table 6 – Comparison between the fuel, flight time, cash operating cost and direct operating cost reference and optimised aircraft for the design mission.

Aircraft	Fuel Consumption	Flight Time	COC	DOC
Reference	1	1	1	1
Optimised	1.11	1.27	1.14	1.20

Table 7 – Comparison between the fuel, flight time, cash operating cost and direct operating cost reference and optimised aircraft for the entire route network.

Aircraft	Fuel Consumption	Flight Time	COC	DOC
Reference	1	1	1	1
Optimised	1.11	1.23	1.13	1.17

For the design mission it is observed that the total fuel consumption of the climate optimised aircraft is 11% higher than the reference aircraft. The flight time increases by 27%, influenced by flying at lower Mach number. The COC and DOC of the climate optimised aircraft are 14% and 20% higher, respectively, than the reference aircraft for the design mission. Table 6 summarises the performance measures for the design mission for reference and optimised aircraft. The values are represented relative to the reference aircraft. In Table 7 the performance indicators are compared for the entire route network. In comparison to the reference aircraft, total network fuel consumption increases by 11% for the total network and the total flight time increases by 23% when operated with optimised aircraft. The COC and DOC increases by 13% and 17%, respectively, when operated on the entire route network.

6. Conclusion and Future Work

This paper presented an efficient methodology for designing next-generation climate-optimal aircraft designs. The proposed method using innovative Climate Functions for Aircraft design can evaluate the climate impact of CO_2 and non-CO_2 effects with high computational efficiency compared to previously used complex climate-chemistry models.

The development methodology of the CFAD implicitly includes the route network information to include the effects of non-CO_2 emissions, which are largely dependent on the atmospheric state. The ATR_{100} is selected as the climate metric to quantify the climate impact. CFAD are developed as a function of climb angle and final cruise altitude to be coupled with the aircraft's multidisciplinary design process. In this study, the representative route network which are operated with aircraft more than 252 seats, was selected for the development of the CFAD. Correspondingly, the A350-900 was selected as the reference aircraft. The climate functions were generated as a 4D response surface model capable of evaluating the climate impact of CO_2, H_2O, NO_x (which influences CH_4, O_3, and PMO [Primary Mode Ozone]), and contrails.

We implemented the CFAD in a multidisciplinary design optimisation framework to demonstrate the application of the CFAD and study the effect of aircraft design choices on the climate impact. First, we investigated the influence of cruise altitude and Mach number on the average temperature

response, considering the selected wide-body, long-range aircraft category. This experiment indicated that flying lower and slower, and adapting the aircraft design accordingly, can reduce ATR_{100} by nearly 40%. Second, we performed a multidisciplinary design optimisation with the CFAD to minimise the climate impact. This optimisation indicated that by reducing the engine overall pressure ratio and adapting the airframe, in addition to the different cruise conditions, the ATR_{100} reduction can be extended to approximately 57%, recognising the remaining uncertainties.

To validate the CFAD, we carried out a higher fidelity assessment. The assessment was performed with the reference aircraft using two different performance models, for three flight levels. It is observed that in general the climate impact is underestimated with the CFAD. At low altitudes, the CFAD can estimate the climate impact with reasonable accuracy. The error in predicting the effects of ozone introduces inaccuracies at high altitudes. However, the relative change in ATR with flight level is similar for both the higher fidelity model and CFAD.

The direct operating cost of the climate-optimised aircraft, discussed in this paper, is 17% higher than the reference aircraft when operated on the entire network. Achieving maximum climate mitigation potential is linked with cost increase. Therefore, a careful consideration of the trade-off between cost and climate mitigation is necessary. A future recommendation for aircraft design studies is to consider multi-objective cost function (climate mitigation vs. operating cost) in conjunction with CFAD. Furthermore, the outcome of flying slower considerably increase the flight time. This is a crucial performance parameter which also needs to be considered within the trade-off analysis.

Further improvements and analysis are required to improve the fidelity of the CFAD at high altitudes. The future development of the CFAD will include updates to the chosen scenarios and utilise improved computational methods. Improving the accuracy of the CFAD is an iterative process, as next step to improving the fidelity a detailed analysis of the underlying assumptions and modelling errors will be carried out. Also, the aircraft design obtained through optimisation does depend on underlying assumptions, such as the relation to estimate the NO_x emission index. We recommend studying the influence of such assumptions on the optimal design. Furthermore, we propose to apply the CFAD in the assessment of new technologies.

7. Copyright Issues

8. Acknowledgements

The project implementing the concept presented in this paper has received funding from the Clean Sky 2 Joint Undertaking under the European Union's Horizon 2020 research and innovation programme under grant agreement No. 865300.

9. Contact Author Email Address

Corresponding Authors: K. Radhakrishnan: kaushik.radhakrishnan@tuhh.de; K. Deck: k.t.deck@tudelft.nl; P. Proesmans: p.proesmans@tudelft.nl

Nomenclature

ATR	Average Temperature Response
CCFs	Climate Change Functions
CFAD	Climate Functions for Aircraft Design
COC	Cash operating cost
DOC	Direct operating cost
FL	Flight Level
GLOWOPT	Global warming optimized aircraft design
ICAO	International Civil Aviation Organisation
IPCC	Intergovernmental Panel on Climate Change
MDO	Multidisciplinary design optimisation
MTOM	Maximum take-off mass
OEM	Operating empty mass
OPR	Overall pressure ratio
PMO	Primary mode ozone
TLAR	Top-level aircraft requirement
TOFL	Take-off field length
XDSM	Extended Design Structure Matrix

References

[1] R. Vos, A. Wortmann, and R. Elmendorp. The optimal cruise altitude of LNG-fuelled turbofan aircraft. *Journal of Aerospace Operations*, 2017.

[2] D. S. Lee, D. W. Fahey, A. Skowron, M. R. Allen, U. Burkhardt, Q. Chen, S. J. Doherty, S. Freeman, P. M. Forster, J. Fuglestvedt, A. Gettelman, R. R. De Leon, L. L. Lim, M. T. Lund, R. J. Millar, B. Owen, J. E. Penner, G. Pitari, M. J. Prather, R. Sausen, and L. J. Wilcox. The contribution of global aviation to anthropogenic climate forcing for 2000 to 2018. *Atmospheric Environment*, 244(117834), 2021.

[3] V. Grewe, A. Stenke, R. Sausen, G. Pitari, D. Lachetti, H. Rogers, O. Dessens, J. Pyle, I. S. A. Isaksen, L. Gulstad, O. A. Søvde, C. Marizy, and E. Pascuillo. Climate impact of supersonic air traffic: an approach to optimize a potential future supersonic fleet – results from the eu-project scenic. *Atmospheric Chemistry and Physics*, 7:5129–5145, 2007.

[4] V. Grewe, M. Plohr, G.Cerino, M. Di. Muzio, Y. Deremaux, M. Galerneau, P. de Saint Martin, T. Chaika ans A. Hasselrot T. U., and V. Korovkin. Estimates of the climate impact of future small-scale supersonic transport aircraft - results from the hisac eu-project. *The Aeronautical Journal*, 114:199–206, 2010.

[5] C. Frömming, M. Ponater, K. Dhalmann, V. Grewe, D.S. Lee, and R. Sausen. Aviation-induced radiative forcing and surface temperature change in dependency of the emission altitude. *Journal of Geophysical Research*, 117:D19, 2012.

[6] V. Grewe, T. Champougny, S. Matthes, C. Frömming, S. Brinkop, O. A. Søvde, E. A. Irvine, and L. Halscheidt. Reduction of the air traffic's contribution to climate change: A REACT4C case study. *Atmospheric Environment*, 94:616–625, 2014.

[7] V. Grewe, C. Frömming, S. Matthes, S. Brinkop, M. Ponater, S. Dietmüller, P. Jöckel, H. Garny, E. Tsati, K. Dahlmann, O. A. Søvde, J. Fuglestvedt, T. K. Berntsen, K. P. Shine, E. A. Irvine, T. Champougny, and P. Hullah. Aircraft routing with minimal climate impact: the REACT4C climate cost function modelling approach (V1.0). *Geoscientific Model Development*, 7:175–201, 2014.

[8] S. Matthes, V. Grewe, K. Dahlmann, C. Frömming, E. A. Irvine, L. Lim, F. Linke, B. Lührs, B. Owen, K. P. Shine, S. Stromatas, H. Yamashita, and F. Yin. A concept for multi-criteria environmental assessment of aircraft trajectories. *Aerospace*, 4(42), 2017.

[9] V. Grewe and K. Dahlmann. How ambiguous are climate metrics? and are we prepared to assess and compare the climate impact of new air traffic technologies? *Atmospheric Environment*, 104:373–374, 2015.

[10] J. S. Fuglestvedt, K. P. Shine, T. Berntsen, J. Cook, D. S. Lee, A. Stenke, R. B. Skeie, G. J. M. Velders, and I. A. Waitz. Transport impacts on atmosphere and climate: Metrics. *Atmospheric Environment*, 44:4648–4677, 2010.

[11] F. Linke. *"Trajectory Calculation Module (Teil I: VNAV)*. PhD thesis, German Aerospace Center, Hamburg, 2008.

[12] V. Grewe and A. Stenke. Airclim: an efficient tool for climate evaluation of aircraft technology. *Atmospheric Chemistry and Physics*, 8(16):4621–4639, 2008.

[13] K. Dahlmann. *Eine Methode zur effizienten Bewertung von Maßnahmen zur Klimaoptimierung des Luftverkehrs*. PhD thesis, Ludwig–Maximilians–Universität München, 2012.

[14] IPCC. Ipcc special report aviation and the global atmosphere, 1999.

[15] IPCC. Ipcc special report emissions scenarios, 2000.

[16] R. Ghosh, K. Kölker, and I. Terekhov. Future passenger air traffic modelling: A theoretical concept to integrate quality of travel, cost of travel and capacity constraints. 19th World Conference of the Air Transport Research Society (ATRS), Singapore, 2015.

[17] A. Koch. *Climate Impact Mitigation Potential Given by Flight Profile and Aircraft Optimization*. PhD thesis, Technische Universität Hamburg-Harburg, Hamburg, Germany, 2013.

[18] U. Schumann, K. Graf, and H. Mannstein. Potential to reduce the climate impact of aviation by ight level changes. 3rd AIAA Atmospheric Space Environments Conference. AIAA paper 2011-3376, 2011.

[19] S. Hartjes, T. Hendriks, and H. G. Visser. Contrail mitigation through 3d aircraft trajectory optimization. 16th AIAA Aviation Technology, Integration, and Operations Conference, American Institute of Aeronautics and Astronautics, 2016.

[20] B. Lührs, M. Niklaß, C. Frömming, V. Grewe, and V. Gollnick. Cost-benefit assessment of 2d and 3d climate and weather optimized trajectories. In Proceedings of the 16th AIAA Aviation Technology, Integration and Operations Conference, 13-17 June 2016. Washington, DC, USA.

[21] B. Lührs, F. Linke, S. Matthes, V. Grewe, and F. Yin. Climate impact mitigation potential of european air traffic in a weather situation with strong contrail formation. *Aerospace*, 8(2), 2021.

[22] K. Dahlmann, A. Koch, F. Linke, B. Lührs, V. Grewe, T. Otten, D. Seider, V. Gollnick, and U. Schumann. Climate-compatible air transport system - climate impact mitigation potential for actual and future aircraft. *Aerospace*, 3:38, 2016.

[23] ICAO. Aerodrome design manual - part 1: Runways, 2006.

[24] P. Proesmans and R. Vos. Airplane design optimization for minimal global warming impact. AIAA Scitech 2021 Forum, Virtual Event, 2021.

[25] E. Torenbeek. *Synthesis of subsonic airplane design*. Delft University Press and Kluwer Academic Publishers, 1 edition, 1982.

[26] D. Raymer. *Aircraft design: a conceptual approach*. American Institute of Aeronautics and Astronautics, 5 edition, 2012.

[27] J.D. Mattingly, W.H. Heiser, and D.T. Pratt. *Aircraft Engine Design*. American Institute of Aeronautics and Astronautics, 2 edition, 2002.

[28] P.P. Walsh and P. Fletcher. *Aircraft Engine Design*. American Institute of Aeronautics and Astronautics, 2 edition, 2002.

[29] E. Torenbeek. The initial calculation of range and mission fuel during conceptual design. Technical Report LR-525, Delft University of Technology, Faculty of Aerospace Engineering, 1987.

[30] E. Dallara and I. Kroo. Aircraft design for reduced climate impact. 49th AIAA Aerospace Sciences Meeting including the New Horizons Forum and Aerospace Exposition, Orlando, Florida, 2011.

[31] M.O. Köhler, G. Rädel, O. Dessens, K.P. Shine, H.L. Rogers, O.Wild, and J.A. Pyle. Impact of perturbations to nitrogen oxide emissions from global aviation. *Journal of Geophysical Research: Atmospheres*, 113(D11), 2008.

[32] G. Rädel and K.P. Shine. Radiative forcing by persistent contrails and its dependence on cruise altitudes. *Journal of Geophysical Research: Atmospheres*, 113(D7):D07105, 2008.

[33] F. Linke. *Environmental Analysis of Operational Air Transportation Concepts*. PhD thesis, Hamburg

University of Technology, Hamburg, 2016.

[34] V. Mouillet. Session 4: Bada family 4 - state of the art. BADA User Group Meeting, EUROCONTROL Experimental Centre, Brétigny sur Orge, France, 2013.

[35] A. Nuic, D. Poles, and V. Mouillet. Bada: An advanced aircraft performance model for present and future atm systems. *nt. J. Adapt. Control Signal Process*, 24:850–866, 2010.

[36] R.H. Liebeck. Advanced subsonic airplane design and economic studies. NASA CR 195443, 1995.